JACS
JOURNAL OF THE AMERICAN CHEMICAL SOCIETY

Article

pubs.acs.org/JACS

Self-Assembly and Photopolymerization of Sub-2 nm One-Dimensional Organic Nanostructures on Graphene

Aparna Deshpande,[†,∥,⊥] Chun-Hong Sham,[†,⊥] Justice M. P. Alaboson,[†] Jonathan M. Mullin,[‡] George C. Schatz,[‡] and Mark C. Hersam[†,‡,§,*]

[†]Department of Materials Science and Engineering, Northwestern University, Evanston, Illinois 60208, United States

[‡]Department of Chemistry, Northwestern University, Evanston, Illinois 60208, United States

[§]Department of Medicine, Northwestern University, Evanston, Illinois 60208, United States

Supporting Information

ABSTRACT: While graphene has attracted significant attention from the research community due to its high charge carrier mobility, important issues remain unresolved that prevent its widespread use in technologically significant applications such as digital electronics. For example, the chemical inertness of graphene hinders integration with other materials, and the lack of a bandgap implies poor switching characteristics in transistors. The formation of ordered organic monolayers on graphene has the potential to address each of these challenges. In particular, functional groups incorporated into the constituent molecules enable tailored chemical reactivity, while molecular-scale ordering within the monolayer provides sub-2 nm templates with the potential to tune the electronic band structure of graphene via quantum confinement effects. Toward these ends, we report here the formation of well-defined one-dimensional organic nanostructures on epitaxial graphene via the self-assembly of 10,12-pentacosadiynoic acid (PCDA) in ultrahigh vacuum (UHV). Molecular resolution UHV scanning tunneling microscopy (STM) images confirm the one-dimensional ordering of the as-deposited PCDA monolayer and show domain boundaries with symmetry consistent with the underlying graphene lattice. In an effort to further stabilize the monolayer, in situ ultraviolet photopolymerization induces covalent bonding between neighboring PCDA molecules in a manner that maintains one-dimensional ordering as verified by UHV STM and ambient atomic force microscopy (AFM). Further quantitative insights into these experimental observations are provided by semiempirical quantum chemistry calculations that compare the molecular structure before and after photopolymerization.

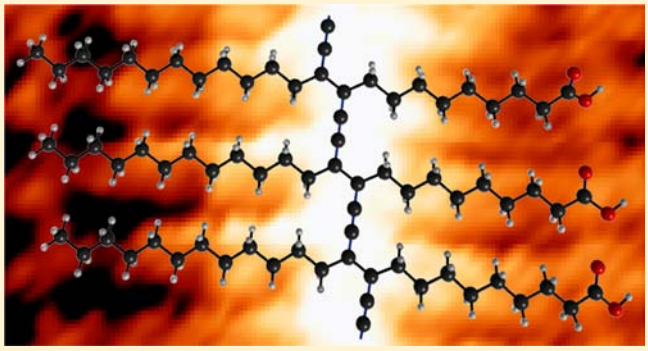

INTRODUCTION

Graphene is a two-dimensional allotrope of sp^2 bonded carbon atoms arranged in a honeycomb lattice.[1] Although graphene was predicted to be a zero bandgap semiconductor from tight binding calculations as early as 1947,[2] experimental study of graphene only became commonplace recently following the isolation of graphene from graphite by mechanical exfoliation using scotch tape.[3] Similarly, epitaxial graphene (EG) grown on silicon carbide (SiC) was first prepared decades ago,[4] but only in the past decade has it been adapted for graphene research.[5,6] Other methods for growing graphene, such as chemical vapor deposition (CVD) on transition metals, have also been developed.[7] While subtle differences exist as a function of synthetic method, graphene is generally endowed with unique properties such as ultrahigh carrier mobility,[1,8,9] intrinsic strength,[10] optical transparency,[11] and thermal conductivity.[12] These superlative properties have begun to be exploited in technologically significant applications, including the recent demonstration of radio frequency (RF) transistors fabricated on wafer-scale EG[13] and CVD graphene.[14] Despite these important developments, its lack of a bandgap, which leads to poor switching behavior in graphene transistors, and its chemical inertness, which introduces challenges in integrating graphene with other materials, have imposed limits on graphene-based device performance, especially in digital electronics.[15,16]

One potential pathway to overcome these issues is surface chemical functionalization of graphene. Covalent modification of graphene with hydrogen,[17−20] oxygen,[21] fluorine,[22,23] and diazonium compounds[24−26] has been shown to open a bandgap in graphene, although typically at the expense of reduced charge carrier mobility. Another path for modulating the band structure of graphene is to form nanoribbons at the sub-5 nm scale.[27,28] Nanoribbons have been formed via oxidative unzipping of carbon nanotubes[29,30] and bottom-up organic

Received: July 19, 2012
Published: August 28, 2012

   dx.doi.org/10.1021/ja307061e | J. Am. Chem. Soc. 2012, 134, 16759−16764

synthesis,[31] but again the resulting electronic devices have lacked the high speed performance of pristine graphene. Alternatively, top-down methods based on organic self-assembled monolayers (SAMs) on graphene have begun to be explored. For example, 3,4,9,10-perylene-tetracarboxylic dianhydride (PTCDA) forms ordered SAMs on epitaxial graphene, uniformly covering the graphene surface without interruption from steps and defects.[32−34] Using ultrahigh vacuum (UHV) scanning tunneling microscopy (STM) lithography, PTCDA has been nanopatterned at the sub-5 nm level and used as a template for subsequent chemical modification of graphene.[35] Furthermore, PTCDA has shown utility as a seeding layer for atomic layer deposition of high-k dielectrics,[36] demonstrating the ability of SAMs to tailor surface chemical reactivity and enable integration of disparate materials with graphene. Similarly, two-dimensional molecular crystals of phosphonic acids have been shown to form on exfoliated graphene, providing a molecular method for doping the underlying graphene.[37]

While the aforementioned early examples of SAMs on graphene have achieved important milestones, the molecular ordering in these cases is essentially isotropic and independent of the underlying graphene lattice. Consequently, it is difficult to imagine these SAMs as templating layers for nanostructuring the underlying graphene with well-defined geometries. In contrast, 10,12-pentacosadiynoic acid (PCDA), $C_{25}H_{42}O_2$, is a photoactive organic molecule[38] that is known to assemble in anisotropic one-dimensional arrays on highly oriented pyrolytic graphite (HOPG)[25−27] and molybdenum disulfide (MoS_2)[42] as shown schematically in Figure 1. PCDA molecular assembly on

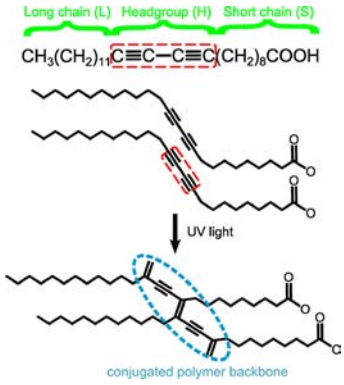

Figure 1. Schematic of 10,12-pentacosadiynoic acid (PCDA) self-assembly and photopolymerization.

HOPG has been previously studied in UHV,[41,43] enabling the formation of PCDA-based SAMs with low defect densities over large areas. The diacetylene core of PCDA also presents opportunities for photopolymerization[44] (see Figure 1), leading to covalent linkages within the monolayer that can improve structural stability at the molecular scale.

Herein, we present a combined UHV STM and computation modeling study of PCDA self-assembly and photopolymerization on EG on SiC(0001). Following deposition in UHV, PCDA is found to assemble into well-ordered one-dimensional structures that show domain boundaries with symmetry consistent with the underlying graphene lattice. Furthermore, the ordering of the PCDA-based SAM faithfully tracks the morphology of the underlying graphene, including seamless transitions over atomic step edges and defects in the underlying SiC substrate. The PCDA monolayer is shown to be stable following removal from UHV, as the one-dimensional anisotropic structure is detected in ambient conditions with AFM. Furthermore, in situ ultraviolet (UV) photopolymerization is achieved, as evidenced by topographic changes in the diacetylene core of PCDA that are detectable by UHV STM and ambient AFM, and are shown to be consistent with semiempirical quantum chemistry calculations. Overall, this study demonstrates that PCDA self-assembly and photopolymerization are compatible with graphene substrates, thus establishing a wafer-scale chemical method for forming well-defined, one-dimensional, sub-2 nm molecular nanostructures on graphene.

EXPERIMENTAL SECTION

Materials. 10,12-Pentacosadiynoic acid (PCDA) (≥97%, Sigma Aldrich) was used as received. The PCDA powder was loaded in an alumina-coated tungsten boat (Midwest Tungsten, AC-32). Prior to filling the boat with PCDA, the boat was resistively heated to degas overnight in a home-built UHV system chamber.[45] 6H-SiC(0001) n-type wafers (Cree) were used to prepare epitaxial graphene. The wafer was cleaned by ultrasonication in acetone and isopropanol followed by degassing at 600 °C for at least 8 h in UHV before graphitization. A 254 nm UV pen lamp (Spectroline 11SC-1) was used as the light source for photopolymerization. The pen lamp was attached to a UV transparent viewport (Nor-Cal, fused silica, diameter = 16.5 mm) on the UHV chamber load lock. During UV exposure, the sample was positioned in the load lock (pressure < 10^{-7} Torr) at a distance of 15 cm from the UV pen lamp.

Epitaxial Graphene Sample Preparation. The SiC sample was graphitized by annealing at 1350 °C for 30 s in UHV for 12 cycles with a 15 min gap between each cycle. The sample was then cooled to room temperature before STM imaging in a home-built STM that was housed in the same UHV chamber with a base pressure of 5×10^{-11} Torr.[45]

Molecular Dosing. After STM imaging of the sample to confirm graphitization, 10,12-pentacosadiynoic acid (PCDA) molecules were sublimated onto the graphene sample in UHV. In particular, the PCDA sublimation boat was resistively heated until the chamber pressure reached 2×10^{-10} to 4×10^{-10} Torr. The epitaxial graphene sample at room temperature was then brought in line of the PCDA flux at a distance of 0.5−1 cm for 15−20 min.

Scanning Tunneling Microscopy. STM imaging was carried out with a home-built STM that possesses a dual concentric piezotube design.[46] Topographic imaging was accomplished in constant current mode with the bias voltage applied to the sample with respect to the electrochemically etched tungsten tip that was grounded through a current preamplifier (DL Instruments, Model 1211). STM imaging was performed after graphitization of the SiC substrate to confirm graphitization and obtain images of the bare graphene surface. These images revealed that the epitaxial graphene samples were atomically clean and consisted of a mixture of monolayer and bilayer graphene.[24] Next, PCDA molecules were deposited onto the graphene surface in UHV according to the procedure described earlier. The resultant surface was imaged by UHV STM, after which the sample was brought to the load lock for UV exposure. Finally, STM images were taken again to confirm and characterize the resulting photopolymerization.

Atomic Force Microscopy. The graphene sample with vapor-deposited PCDA molecules was taken out of the UHV chamber for subsequent ambient AFM studies. AFM imaging was performed both before and after polymerization. AFM images were collected with a CP Research AFM (Thermomicroscopes) in air. Imaging was performed in intermittent contact mode using an Si probe (μMasch, NSC36A) with a nominal tip radius of curvature of 10 nm. AFM images were rendered using WSxM SPM analysis software.[47]

Computational Details. The PCDA molecule assembly structures were optimized using a neglect of diatomic differential overlap method, PM6 (Parameterized Model number 6).[48] PM6 is a semiempirical

dx.doi.org/10.1021/ja307061e | J. Am. Chem. Soc. 2012, 134, 16759−16764

method where the optimization was done with a tolerance of 10^{-4} in the gradient as implemented in MOPAC (Molecular Orbital PACkage). The visualizations were accomplished with MacMolPlot.[49]

RESULTS

UHV STM of PCDA before Polymerization. STM images of the epitaxial graphene substrate after vapor deposition of PCDA are shown in Figure 2. In the large-scale image in Figure 2a, the molecules are observed to self-assemble into one-dimensional stripes. The stripes are observed to seamlessly cross the steps and terraces of the underlying epitaxial graphene and SiC. The molecular structure of these one-dimensional stripes is revealed in the high-resolution STM image in Figure 2b. The stripes consist of bright headgroups (H) with a short chain (S) and a long chain (L) on either side of the headgroup. In other words, one molecule is indicated by 1 unit of "SHL" in Figure 2. The bright headgroup is assigned to the central diacetylene portion of the PCDA molecule. The short chain is terminated by a carboxylic group that is hydrogen bonded to the carboxylic group on the neighboring PCDA molecule. Finally, the long chain is the methyl-terminated alkyl chain of the PCDA molecule. The molecules self-assemble in the repeating pattern "SHL−LHS," forming a 7.5 ± 0.3 nm wide unit cell as shown in Figure 2b. This "SHL-LHS" ordering of PCDA on graphene is consistent with the assembly of PCDA molecules on HOPG observed by STM in ambient,[39] in UHV,[41] and at the liquid−solid interface.[50] However, in contrast to HOPG, the PCDA ordering is observed to be generally unhindered by the step edges and terraces of the epitaxial graphene and underlying SiC.

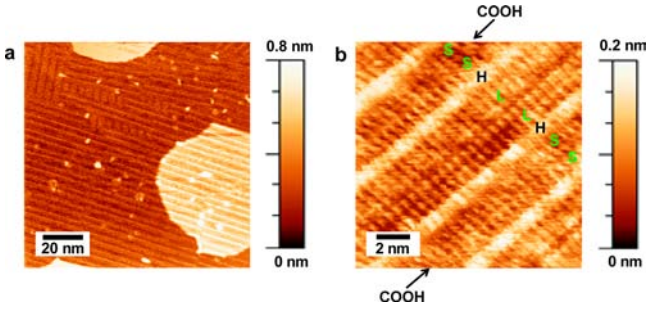

Figure 2. (a) Large-area STM image of PCDA on epitaxial graphene. Imaging conditions: sample bias = 1 V; tunneling current = 100 pA. (b) High-resolution STM image of PCDA on epitaxial graphene. Imaging conditions: sample bias = 0.5 V; tunneling current = 800 pA. The intramolecular PCDA structure is labeled with H for the central diacetylene headgroup, S for the short carboxylic-terminated alkyl chain, and L for the long methyl-terminated alkyl chain.

UHV STM of PCDA after UV Photopolymerization. STM images of PCDA molecules after UV photopolymerization are shown in Figure 3. One-dimensional protrusions less than 2-nm wide are observed and are marked by red arrows in Figure 3a. These photopolymerized chains traverse seamlessly over step edges and appear higher and brighter than the neighboring unpolymerized PCDA molecules. In Figure 3b, a high-resolution STM image reveals the molecular structure of the conjugated backbone following photopolymerization. Averaging multiple measurements, the height difference between polymerized and unpolymerized PCDA molecules is 1.15 ± 0.56 Å, as outlined in detail in the Supporting Information. In contrast to PCDA on HOPG and MoS_2, this measured height difference is independent of sample bias between −1 and 1 V.[42] In addition to the increase in height following photopolymerization, a change in the angle of the side chains with respect to the one-dimensional ordering direction is also observed. This change in angle is most easily observed in the high-resolution STM image in Figure 3b. The change in the angle was measured to be (15.5 ± 5.5)°, consistent with the reported (12 ± 2) ° on HOPG.[40]

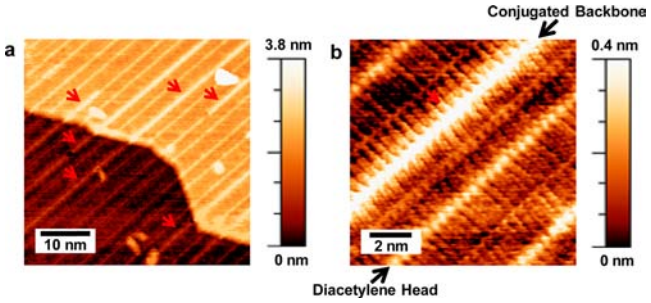

Figure 3. (a) Large-area STM image after UV photopolymerization of PCDA on epitaxial graphene. Imaging conditions: sample bias = 0.7 V; tunneling current = 227 pA. (b) High-resolution STM image recorded with the same imaging parameters as in (a). The photopolymerized conjugated backbone is raised in height with respect to adjacent unpolymerized PCDA molecules.

As seen in Figure 4, the PCDA molecules are observed to self-assemble into domains that possess angles that are approximately commensurate with the symmetry of the underlying graphene substrate. A histogram of angles from several STM images is plotted in Figure 4b. The maxima occur at 10°, 65°, and 120°. The small offset from the 60° symmetry axes of the graphene lattice highlights the competitive nature of intermolecular interactions compared to molecule−substrate interactions and is similar to observations previously reported for PCDA on HOPG and MoS_2.[42] It should be noted that the orientation of the PCDA stripes is observed to change after repeated scanning, reflecting relatively weak interaction with the underlying graphene substrate. However, the clear peaks in the angular histogram at multiples of ~60° suggest a registry with the underlying graphene that is analogous to previous observations on HOPG.[39] This registry is considerably closer than previously studied organic self-assembled monolayers on graphene such as PTCDA.[32,33]

Atomic Force Microscopy Measurements. In an effort to assess the stability and large-area uniformity of the PCDA self-assembled monolayer, the PCDA-coated epitaxial graphene sample was taken out of UHV to the ambient environment where AFM imaging was performed at multiple locations across the sample. On the as-deposited PCDA samples (i.e., preceding photopolymerization), the AFM images (Figure 5) show highly ordered stripes over the entire sample that share similarities with the previously discussed UHV STM images. In particular, the pitch of the stripes is found to be 7.3 ± 0.3 nm, which is in close agreement with the length of two adjacent PCDA molecules in the STM images. However, considering the two-molecule pitch between the stripes observed in the AFM images, one elevated stripe in AFM corresponds to a stripe pair observed in STM. Consequently, the elevated stripes observed in AFM are assigned to the carboxylic end groups, in agreement with an earlier AFM study of PCDA on HOPG.[51] The topography of PCDA molecules as observed by AFM is different from STM due to the additional density of states imaging contrast provided during STM imaging, where the

dx.doi.org/10.1021/ja307061e | J. Am. Chem. Soc. 2012, 134, 16759−16764

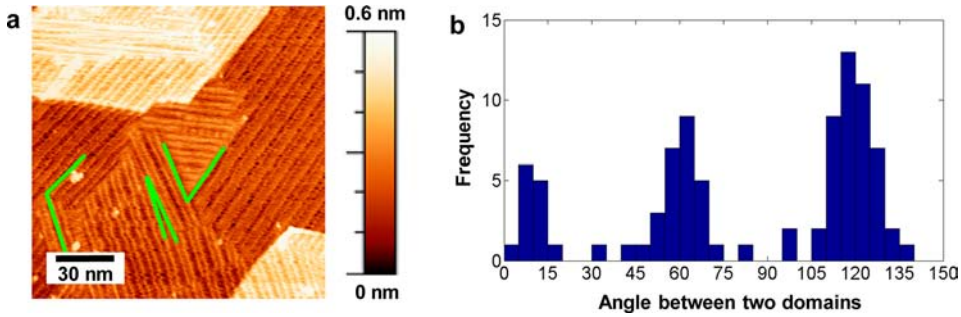

Figure 4. (a) STM image showing the angular orientation at PCDA domain boundaries. Imaging conditions: sample bias = 1 V; tunneling current = 100 pA. (b) Histogram of different domain angles extracted from several STM images.

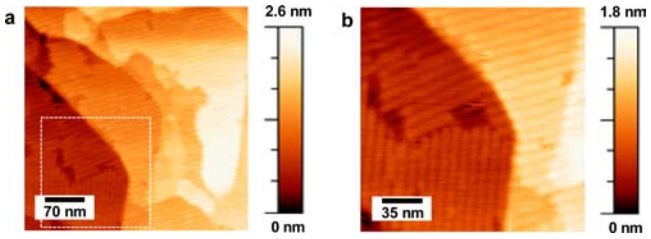

Figure 5. (a) Large-area intermittent contact AFM image of as-deposited PCDA molecules (i.e., preceding photopolymerization) on epitaxial graphene. (b) High-resolution intermittent contact AFM image of the region outlined with the white dashed square shown in (a).

diacetylene head groups appear as bright protrusions and the carboxylic groups appear as depressions. For this reason, the AFM images do not exhibit the "LHS" ordering as seen in the previous STM images.[29] Nevertheless, it is apparent from AFM that the ordering of PCDA molecules on epitaxial graphene is stable outside of UHV in ambient conditions.

The as-deposited PCDA sample subsequently underwent UV photopolymerization in the load lock at a pressure below 10^{-7} Torr for 1 h and then was reimaged using ambient AFM, as shown in Figure 6. After UV photopolymerization, the AFM

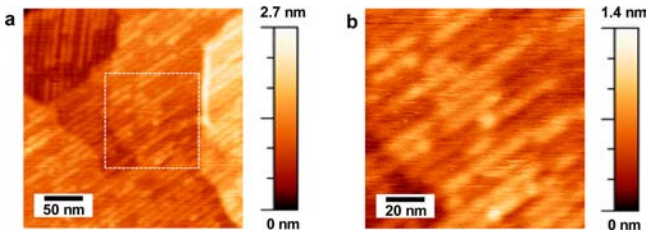

Figure 6. (a) Large-area intermittent contact AFM image of photopolymerized PCDA molecules on epitaxial graphene. (b) High-resolution intermittent contact AFM image of the region outlined with the white dashed square shown in (a).

images reveal that certain stripes appear elevated compared to their neighbors, in agreement with the previous discussed UHV STM images. AFM height profiles taken across the protruding stripes show a height increase of (2.5 ± 1.0) Å with respect to neighboring stripes. The presence and the height of the protruding stripes are in agreement with previous AFM studies of PCDA on HOPG following UV irradiation.[51]

Computational Results. The PCDA conformers were each modeled with the semiempirical PM6 model, which neglects diatomic differential overlap. The conformer calculations consisted of 10 "monomer" substituents aligned in a plane. The Z coordinate of the carbon atoms in the optimization was held fixed to approximate the effects of binding to a graphene substrate. Each of the conformers was found to be a local energy minimum. Figure 7a shows an array of PCDA molecules preceding photopolymerization. Following photopolymerization (here the Z coordinate is not fixed), the PCDA molecular array has two forms: (1) a flat polymer where the diacetylene backbone is not raised, as shown in Figure 7b, and the raised polymer with the raised diacetylene backbone, as shown in Figure 7c. In Figure 7a–c, one "monomer" has the carbon atoms numbered. A comparison of the relative angles of the polymeric forms (Figure 7b,c) compared to the monomeric form (Figure 7a) allows identification of the polymerized structure in the STM images. These angles are defined by atoms 1–13–16 for the methyl-terminated end and by atoms 13–16–25 for the carboxylic end. The values presented here are an average over eight angles excluding each molecule on the edges to avoid artifacts of the finite structure. The relative angle difference was 4° for the flat polymer (Figure 7b), and 10° for the buckled polymer (Figure 7c).

■ DISCUSSION

Diacetylene monomers are known to undergo polymerization upon exposure to UV light in solution. In this work, photopolymerization of a diacetylene-based compound, PCDA (10,12-pentacosadiynoic acid), was demonstrated and monitored on epitaxial graphene. In previous studies on substrates such as HOPG, the molecular self-assembly of PCDA was achieved via solution deposition, either through Langmuir–Blodgett[39] (LB) techniques or drop casting[40,42] a solution of PCDA dissolved in a solvent such as chloroform.[42] In contrast, we focused on PCDA deposited from the gas phase in UHV in an effort to minimize contamination. Using this deposition scheme, PCDA was found to self-assemble with one-dimensional ordering on epitaxial graphene (Figure 2a,b). The short alkyl chain attached to the diacetylene unit terminates with a carboxyl group. The carboxyl groups of adjacent PCDA molecules participate in hydrogen bonding between adjacent molecules that helps stabilize the molecular assembly.

Upon UV exposure, the central diacetylene units photopolymerize to form a covalently linked molecular assembly (Figure 3a). The photopolymerization mechanism has previously been attributed to a chain reaction initiated by the formation of a diradical in the diacetylene unit due to photoabsorption.[39] Following photopolymerization, the conjugated backbone shows a height increase of (1.15 ± 0.56) Å in the STM images (Figure 3a,b). This increase in height is

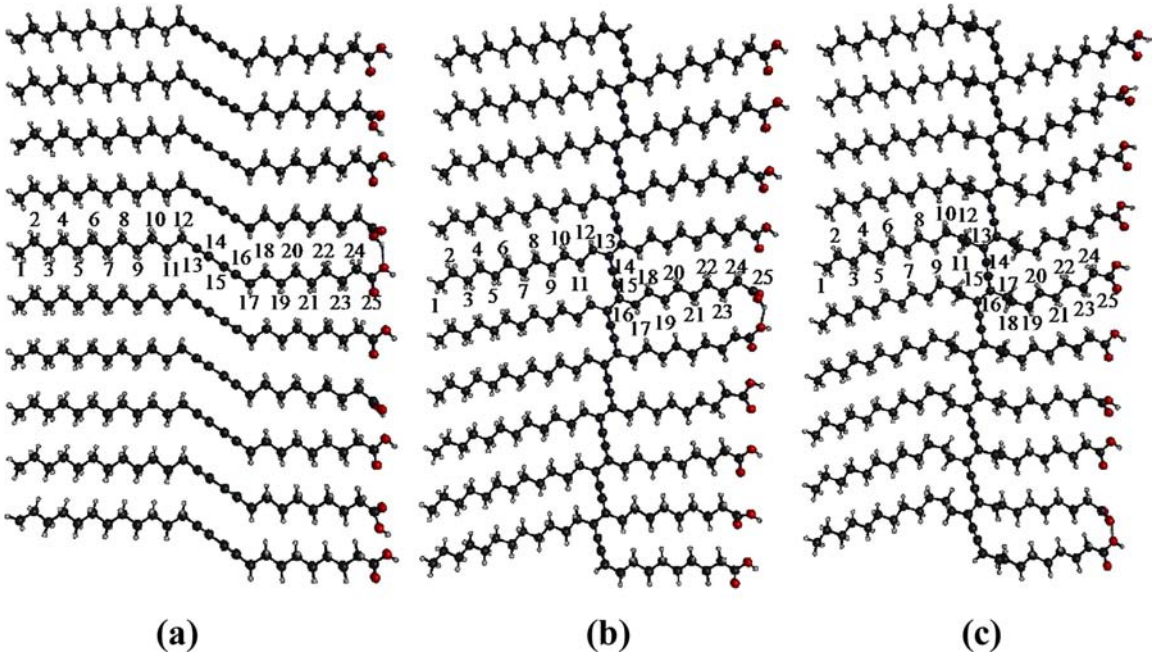

Figure 7. Gas phase PM6 modeling of PCDA molecules showing (a) an array of 10 monomers of PCDA. The carbon atoms of one monomer are numbered for reference to measure the change in the angle of the monomer following polymerization. (b) An array of 10 flat (i.e., in-plane) PCDA polymers. (c) An array of 10 buckled (i.e., raised) polymers.

consistent with an out-of-plane distortion along the polydiacetylene backbone.[51] Photopolymerization is also observed to lead to a change in the angle of the PCDA side chains of $(15.5 \pm 5.5)^\circ$. To gain more insight into the measured changes in height and angle, a semiempirical quantum chemical PM6 method was employed to find the energetically stable structure for the PCDA molecular assemblies before and after photopolymerization. Computationally, two stable polymerized structures are plausible: (1) a flat conformation where the central conjugated backbone remains in plane; (2) a buckled conformation where the central conjugated backbone is raised out of plane. The computational results predict a difference in side chain angle for these two cases: (1) 4° for the flat polymer (Figure 7b); (2) 10° for the buckled polymer (Figure 7c). Although it is difficult to completely rule out a small population of in-plane polymer species, the measured change in height and angle from the STM images following photopolymerization agrees best with the buckled polymer conformation. Figure 8 illustrates this strong correlation between experiment and theory for the buckled polymer conformation.

AFM images of PCDA on epitaxial graphene both before and after photopolymerization are in agreement with previous measurements on HOPG.[51] Importantly, the ambient AFM data reveal the high stability and robustness of the PCDA molecular assembly. This high stability in ambient conditions will provide considerable flexibility in future work aimed at using ordered molecular assemblies on graphene as a template for subsequent chemistry.

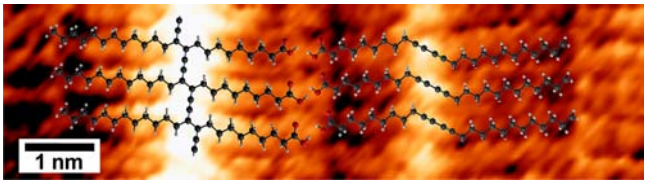

Figure 8. STM image of PCDA monomers (right) and polymers (left) with calculated monomer (right) and buckled polymer (left) structures superimposed on the STM image.

CONCLUSIONS

In summary, room temperature UHV STM, ambient AFM, and semiempirical PM6 calculations were used to investigate the photoactive self-assembly of PCDA on epitaxial graphene. UHV STM imaging provides intramolecular spatial resolution information about the structure and ordering of the resultant molecular assembly, including an apparent high degree of registry between the one-dimensional PCDA assemblies and the underlying graphene lattice. PCDA molecular deposition and UV photopolymerization were achieved in vacuum with the photopolymerized PCDA assemblies showing an increase in height and a change in the side chain angle in constant current STM images. The semiempirical PM6 calculations yielded structures for the PCDA monomer and buckled polymer conformations that quantitatively agreed with the STM data. In addition, ambient AFM characterization demonstrated high stability and robustness for the PCDA assemblies, suggesting their potential use as a template for subsequent chemistry. Given the technological significance of epitaxial graphene and ongoing worldwide efforts to experimentally realize graphene nanoribbons, the highly ordered, one-dimensional, sub-2 nm conjugated PCDA polymers demonstrated here may prove to be useful intermediates or chemical templates/resists for massively parallel, high-resolution nanopatterning of graphene.

ASSOCIATED CONTENT

Supporting Information

Detailed description of the measurement of the height difference between PCDA polymers and monomers. This material is available free of charge via the Internet at http://pubs.acs.org.

dx.doi.org/10.1021/ja307061e | J. Am. Chem. Soc. 2012, 134, 16759−16764

AUTHOR INFORMATION

Corresponding Author

m-hersam@northwestern.edu

Present Address

[‖]Indian Institute of Science Education and Research, Pashan, Pune 411021, India.

Author Contributions

[⊥]These authors contributed equally to this work.

Notes

The authors declare no competing financial interest.

ACKNOWLEDGMENTS

This work was supported by the Department of Energy (Award No. DE-FG02-09ER16109), the Office of Naval Research (Award No. N00014-11-1-0463), and a W. M. Keck Foundation Science and Engineering Grant. The authors thank Joseph Lyding for the use of his STM control software.

REFERENCES

(1) Geim, A. K.; Novoselov, K. S. *Nat. Mater.* **2007**, *6*, 183−191.
(2) Wallace, P. R. *Phys. Rev.* **1947**, *71*, 622−634.
(3) Novoselov, K. S. *Science* **2004**, *306*, 666−669.
(4) Van Bommel, A. J.; Crombeen, J. E.; Van Tooren, A. *Surf. Sci.* **1975**, *48*, 463−472.
(5) Berger, C.; Song, Z.; Li, T.; Li, X.; Ogbazghi, A. Y.; Feng, R.; Dai, Z.; Marchenkov, A. N.; Conrad, E. H.; First, P. N.; Heer, W. A. D. *J. Phys. Chem. B* **2004**, *108*, 19912−19916.
(6) Riedl, C.; Coletti, C.; Starke, U. *J. Phys. D: Appl. Phys.* **2010**, *43*, 374009.
(7) Bae, S.; Kim, H.; Lee, Y.; Xu, X.; Park, J.-S.; Zheng, Y.; Balakrishnan, J.; Lei, T.; Kim, H. R.; Song, Y. I.; Kim, Y.-J.; Kim, K. S.; Ozyilmaz, B.; Ahn, J.-H.; Hong, B. H.; Iijima, S. *Nat. Nanotechnol.* **2010**, *5*, 574−578.
(8) Bolotin, K.; Sikes, K.; Jiang, Z.; Klima, M.; Fudenberg, G.; Hone, J.; Kim, P.; Stormer, H. *Solid State Commun.* **2008**, *146*, 351−355.
(9) Castro Neto, A. H.; Peres, N. M. R.; Novoselov, K. S.; Geim, A. K. *Rev. Mod. Phys.* **2009**, *81*, 109−162.
(10) Lee, C.; Wei, X.; Kysar, J. W.; Hone, J. *Science* **2008**, *321*, 385−388.
(11) Nair, R. R.; Blake, P.; Grigorenko, A. N.; Novoselov, K. S.; Booth, T. J.; Stauber, T.; Peres, N. M. R.; Geim, A. K. *Science* **2008**, *320*, 1308.
(12) Cai, W.; Moore, A. L.; Zhu, Y.; Li, X.; Chen, S.; Shi, L.; Ruoff, R. S. *Nano Lett.* **2010**, *10*, 1645−1651.
(13) Lin, Y.-M.; Dimitrakopoulos, C.; Jenkins, K. A.; Farmer, D. B.; Chiu, H.-Y.; Grill, A.; Avouris, P. *Science* **2010**, *327*, 662.
(14) Wu, Y.; Lin, Y.; Bol, A. A.; Jenkins, K. A.; Xia, F.; Farmer, D. B.; Zhu, Y.; Avouris, P. *Nature* **2011**, *472*, 74−78.
(15) Schwierz, F. *Nat. Nanotechnol.* **2010**, *5*, 487−496.
(16) Schwierz, F. *Science* **2011**, *472*, 41.
(17) Elias, D. C.; Nair, R. R.; Mohiuddin, T. M. G.; Morozov, S. V.; Blake, P.; Halsall, M. P.; Ferrari, A. C.; Boukhvalov, D. W.; Katsnelson, M. I.; Geim, A. K.; Novoselov, K. S. *Science* **2009**, *323*, 610−613.
(18) Guisinger, N. P.; Rutter, G. M.; Crain, J. N.; First, P. N.; Stroscio, J. A. *Nano Lett.* **2009**, *9*, 1462−1466.
(19) Balog, R.; Jørgensen, B.; Wells, J.; Laegsgaard, E.; Hofmann, P.; Besenbacher, F.; Hornekaer, L. *J. Am. Chem. Soc.* **2009**, *131*, 8744−8745.
(20) Sessi, P.; Guest, J. R.; Bode, M.; Guisinger, N. P. *Nano Lett.* **2009**, *9*, 4343−4347.
(21) Hossain, Md. Z.; Johns, J. E.; Bevan, K. H.; Karmel, H. J.; Liang, Y. T.; Yoshimoto, S.; Mukai, K.; Koitaya, T.; Yoshinobu, J.; Kawai, M.; Lear, A. M.; Kesmodel, L. L.; Tait, S. L.; Hersam, M. C. *Nat. Chem.* **2012**, *4*, 305−309.
(22) Cheng, S.-H.; Zou, K.; Okino, F.; Gutierrez, H. R.; Gupta, A.; Shen, N.; Eklund, P. C.; Sofo, J. O.; Zhu, J. *Phys. Rev. B* **2010**, *81*, 205435.
(23) Robinson, J. T.; Burgess, J. S.; Junkermeier, C. E.; Badescu, S. C.; Reinecke, T. L.; Perkins, F. K.; Zalalutdniov, M. K.; Baldwin, J. W.; Culbertson, J. C.; Sheehan, P. E.; Snow, E. S. *Nano Lett.* **2010**, *10*, 3001−3005.
(24) Hossain, Md. Z.; Walsh, M. A.; Hersam, M. C. *J. Am. Chem. Soc.* **2010**, *132*, 15399−15403.
(25) Bekyarova, E.; Itkis, M. E.; Ramesh, P.; Berger, C.; Sprinkle, M.; de Heer, W. A.; Haddon, R. C. *J. Am. Chem. Soc.* **2009**, *131*, 1336−1337.
(26) Sharma, R.; Baik, J. H.; Perera, C. J.; Strano, M. S. *Nano Lett.* **2010**, *10*, 398−405.
(27) Pisani, L.; Chan, J.; Montanari, B.; Harrison, N. *Phys. Rev. B* **2007**, *75*, 064418.
(28) Son, Y. W.; Cohen, M. L.; Louie, S. G. *Phys. Rev. Lett.* **2006**, *97*, 216803.
(29) Kosynkin, D. V.; Higginbotham, A. L.; Sinitskii, A.; Lomeda, J. R.; Dimiev, A.; Price, B. K.; Tour, J. M. *Nature* **2009**, *458*, 872−876.
(30) Jiao, L.; Zhang, L.; Wang, X.; Diankov, G.; Dai, H. *Nature* **2009**, *458*, 877−880.
(31) Cai, J.; Ruffieux, P.; Jaafar, R.; Bieri, M.; Braun, T.; Blankenburg, S.; Muoth, M.; Seitsonen, A. P.; Saleh, M.; Feng, X.; Mullen, K.; Fasel, R. *Nature* **2010**, *466*, 470−473.
(32) Wang, Q. H.; Hersam, M. C. *Nat. Chem.* **2009**, *1*, 206−211.
(33) Emery, J. D.; Wang, Q. H.; Zarrouati, M.; Fenter, P.; Hersam, M. C.; Bedzyk, M. J. *Surf. Sci.* **2011**, *605*, 1685−1693.
(34) Huang, H.; Chen, S.; Gao, X.; Chen, W.; Wee, A. T. S. *ACS Nano* **2009**, *3*, 3431−3436.
(35) Wang, Q. H.; Hersam, M. C. *Nano Lett.* **2011**, *11*, 589−593.
(36) Alaboson, J. M. P.; Wang, Q. H.; Emery, J. D.; Lipson, A. L.; Bedzyk, M. J.; Elam, J. W.; Pellin, M. J.; Hersam, M. C. *ACS Nano* **2011**, 5223−5232.
(37) Prado, M. C.; Nascimento, R.; Moura, L. G.; Matos, M. J. S.; Mazzoni, M. S. C.; Cancado, L. G.; Chacham, H.; Neves, B. R. A. *ACS Nano* **2011**, *5*, 394−398.
(38) Kamath, M.; Kim, W. H.; Li, L.; Kumar, J.; Tripathy, S.; Babu, K. N.; Talwar, S. S. *Macromolecules* **1993**, *26*, 5954−5958.
(39) Okawa, Y.; Aono, M. *J. Chem. Phys.* **2001**, *115*, 2317−2322.
(40) Qiao, Y.-H.; Zeng, Q.-D.; Tan, Z.-Y.; Xu, S.-D.; Wang, D.; Wang, C.; Wan, L.-J.; Bai, C.-L. *J. Vac. Sci. Technol. B* **2002**, *20*, 2466−2469.
(41) Giridharagopal, R.; Kelly, K. F. *J. Phys. Chem. C* **2007**, *111*, 6161−6166.
(42) Giridharagopal, R.; Kelly, K. F. *ACS Nano* **2008**, *2*, 1571−1580.
(43) Kasaya, M. A.; Shimizu, K.; Watanabe, Y.; Saito, A.; Aono, M.; Kuwahara, Y. *Phys. Rev. Lett.* **2003**, *91*, 255501.
(44) Saito, A.; Urai, Y.; Itoh, K. *Langmuir* **1996**, *12*, 3938−3944.
(45) Foley, E. T.; Yoder, N. L.; Guisinger, N. P.; Hersam, M. C. *Rev. Sci. Instrum.* **2004**, *75*, 5280−5287.
(46) Brockenbrough, R.; Lyding, J. W. *Rev. Sci. Instrum.* **1993**, *64*, 2225−2228.
(47) Horcas, I.; Fernández, R.; Gómez-Rodríguez, J. M.; Colchero, J.; Gómez-Herrero, J.; Baro, A. M. *Rev. Sci. Instrum.* **2007**, *78*, 013705.
(48) Stewart, J. J. P. *J. Mol. Model.* **2007**, *13*, 1173−1213.
(49) Bode, B. M.; Gordon, M. S. *J. Mol. Graph. Model.* **1998**, *16*, 133−138.
(50) Takajo, D.; Okawa, Y.; Hasegawa, T.; Aono, M. *Langmuir* **2007**, *23*, 5247−5250.
(51) Okawa, Y.; Takajo, D.; Tsukamoto, S.; Hasegawa, T.; Aono, M. *Soft Matter* **2008**, *4*, 1041−1047.